

Investigation of Polymer Melt Relaxation Mechanisms via Dynamic Infrared Dichroism

Wanda J. Walczak and Richard P. Wool*

Department of Materials Science and Engineering, University of Illinois,
1304 West Green Street, Urbana, Illinois 61801

Received July 31, 1990; Revised Manuscript Received December 21, 1990

ABSTRACT: Single polarization dynamic infrared dichroism is used to investigate the local orientation dynamics of a centrally labeled (HDH) triblock polystyrene (48 400 HPS-66 700 DPS-63 400 HPS) in its homopolymer melt, as it relaxes from a uniaxial step strain. Simultaneous measurement of stress relaxation allows a test of the stress optical law and indicates the relaxation region in which orientation loss of the different chain parts occurs. When the chain ends relaxed from a draw ratio of 2.2 at 125 °C, they were found to relax at the same rate as the chain center in the terminal relaxation region. Chain orientation relaxation by a purely reptative mechanism predicts that the chain ends relax before the chain center. Relaxation of the HDH triblock chain in a higher molecular weight (400 000) matrix showed that the center relaxed more slowly than in the homopolymer. The results are discussed in terms of several relaxation mechanisms involving (1) Rouse relaxation of entanglements, (2) chain retraction, (3) chain end fluctuations, (4) constraint release, (5) reptation, (6) nematic ordering, and (7) percolation of entanglement networks.

Introduction

The purpose of this paper is to analyze molecular orientation relaxation mechanisms during stress relaxation of a polymer film in the melt following a uniaxial step strain. Several relaxation mechanisms have been proposed to explain how a polymer chain in the melt relieves its stress from a uniaxial step strain to achieve an isotropic configuration (Figure 1). These include the following: (a) Rouse relaxation between entanglements (equilibration of monomer density between entanglement points);^{1,2} (b) monomer density equilibration by Rouse motion of the whole chain (retraction resulting in curvilinear chain length equilibration);²⁻⁷ (c) chain length fluctuation (breathing motion of chain length allowing additional relaxation without center-of-mass motion);⁸ (d) reptation^{3,9} (disengagement by curvilinear diffusion from the initially deformed tube to attain an equilibrium isotropic conformation); (e) tube renewal or constraint release¹⁰⁻¹² (reptation of surrounding chains, which leads to the disappearance of topological constraints); (f) nematic coupling^{3,13} (orientation coupling of relaxing chain segments with the surrounding matrix orientation); (g) vector percolation¹⁴ (multichain cooperative relaxation process of a strained entanglement network, which relaxes to zero stress at the percolation threshold) proposed by R.P.W.,¹⁴ and (f) double reptation¹⁵ (entanglement relaxation involves segments from two chains).

In this paper, we describe experiments that simultaneously monitor bulk stress relaxation and molecular orientation relaxation via single polarization infrared dichroism. Three experiments were done with atactic polystyrene melts. The first concerns a completely hydrogenated 233 000 molecular weight polystyrene (HPS) in its homopolymer melt. This experiment probes the molecular orientation relaxation behavior of the average entire polymer chain and compares it to its bulk modulus relaxation. The second experiment involves a centrally deuterated polystyrene (HDH) triblock polymer with a molecular weight of 178 500 (equivalent HPS molecular weight of 173 700). This is done to measure the orientation relaxation of the chain center versus its ends and compare results with the stress relaxation modulus and molecular dynamics theories. The third experiment involves the relaxation of triblock HDH chains in a higher molecular

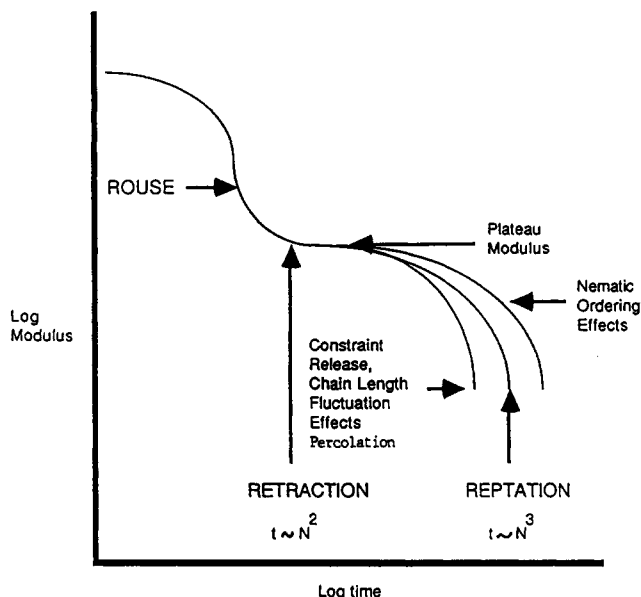


Figure 1. Sketch of the melt relaxation modulus indicating several molecular relaxation mechanisms for a chain of molecular weight N .

weight (400 000) PS matrix. The object of this experiment is to explore matrix effects on the relaxation of individual chain segments. The results are discussed in terms of the proposed relaxation mechanisms and experimental results of other investigators.

Infrared Dichroism

Polarized infrared spectroscopy, or infrared dichroism, is an established tool for studying orientation in polymer melts. If the electric vector of incident radiation, \mathbf{E} , is parallel to the transition dipole moment vector \mathbf{M} , caused by the change in the dipole moment vector upon vibration, then the absorption intensity, A , of this vibration is a maximum. If the electric vector is perpendicular to the transition dipole moment vector, the absorbance is a minimum. Thus

$$A \sim ((\mathbf{M} \cdot \mathbf{E}))^2 = K \cos^2 \alpha \quad (1)$$

where A is the absorbance, α is the angle between \mathbf{M} and

E , and K is a constant independent of orientation. The absorbance measured is an average over all orientations of the particular vibration in the polymer system sampled. The dichroic ratio, R , is defined by

$$R = A_{\parallel}/A_{\perp} \quad (2)$$

which is the ratio of the absorbance measured with parallel polarized light A_{\parallel} , to perpendicularly polarized light, A_{\perp} . R can be related to the second moment of the orientation function, $\langle P_2(\cos \Theta) \rangle$ by the Hermans orientation function f

$$f = 1/2(3\langle \cos^2 \Theta \rangle - 1) \quad (3)$$

such that

$$f = (R - 1)(R_0 + 2)/(R + 2)(R_0 - 1) \quad (4)$$

Here Θ is the average angle between the chain backbone axis and the stretch direction and $R_0 = 2 \cot^2 \alpha$, where α is the angle between the dipole moment vector of vibration and the chain axis.

The relation for the total unpolarized absorbance A_0 in samples with cylindrical symmetry is given by

$$A_0 = (2A_{\perp} + A_{\parallel})/3 \quad (5)$$

By use of this relation, the normalized Hermans orientation function, $F = f/f(\text{initial})$ becomes

$$F = [A_0 - A_{\perp}(t)]/[A_0 - A_{\perp}(i)] \quad (6)$$

where $A_{\perp}(t)$ is the perpendicular absorbance measured at time t after stretching, and $A_{\perp}(i)$ is the perpendicular absorbance measured immediately after stretching. Furthermore, if complete relaxation is achieved, the relation

$$A_0 = A_{\perp} = A_{\parallel} \quad (7)$$

can be used. Measurement of the orientation function is thus reduced to monitoring a single polarization absorbance throughout time by using the equation

$$F = [A(f) - A_{\perp}(t)]/[A(f) - A_{\perp}(i)] \quad (8)$$

where $A(f)$ is the final relaxed perpendicular absorbance.

The static experimental methods used in studying relaxation of uniaxially oriented polystyrene by Lee and Wool¹⁶⁻¹⁸ as well as Monnerie et al.^{5,19-21} required absorbance measurement with both parallel and perpendicularly polarized light. In order to achieve this, the relaxation had to be quenched periodically and subsequently restarted. This experimental method could adversely affect the measurement of a true orientation and its relation with stress. The single polarization method used in situ avoids any errors induced by quenching and allows the simultaneous measurement of stress relaxation. Simultaneous measurement of stress is also desirable since it would indicate at what time and during which relaxation mechanism the changes in orientation occur.

Experimental Procedure

Sample Preparation. Two types of samples were used in the dichroism relaxation experiments. Fully hydrogenated polystyrene, $M_w = 233\,000$, Lot No. 50124, with polydispersity less than 1.06 was purchased from Pressure Chemical. This was used to establish how the orientation relaxation of the entire chain would compare to the sample's bulk modulus relaxation. A centrally deuterated polystyrene with $M_w = 173\,700$ and polydispersity less than 1.04 was purchased from Polymer Labs. This was used to determine how orientation relaxation of different parts of the chain compared with the bulk modulus relaxation. The molecular weight of the different blocks in the centrally deuterated polystyrene was 48 400 HPS-61 900 DPS-63 400 HPS,

Table I
HDH Triblock Molecular Weights

block	M_w	polydispersity	assigned block length	segment length
H	46 687	1.024	48 400	48 400
HD	109 553	1.013	110 300	61 900 (equiv)
HDH	173 658	1.036	173 700	63 400

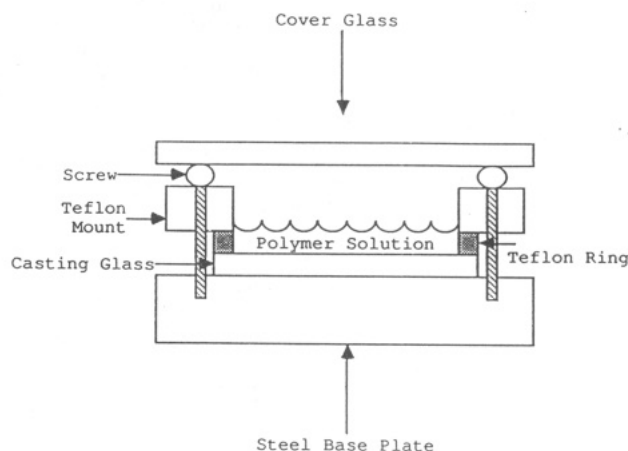


Figure 2. Solution casting mold.

as shown in Table I. The GPC analysis indicated that the HDH triblock was contaminated with a small amount (less than 3%) of the HD diblock with $M \approx 100\,000$, but contained essentially none of the first block ($M \approx 48\,000$). The presence of the diblock was not considered a problem in the analysis. The actual molecular weight of the triblock was 178 500. However, in all calculations of relaxation times we use the equivalent HPS molecular weight of 173 700 by correcting (104/112) for the D_8 deuterated central section.

To make the film samples, 0.42 g of the polymer was first dissolved in 21 mL of Mallinckrodt reagent grade benzene. The sample was dissolved and equilibrated at room temperature for 1 day and filtered twice with Millipore filters with 0.05-mm pore size. The filtered solution was then used to cast 2.5 in. \times 2.5 in. films in a solution casting mold on a level surface, as shown in Figure 2. The solution evaporated in the mold under a moderately ventilated hood after approximately 12 h. Once the solvent evaporated, the sample was cut from the mold by a fresh razor, paper clipped to a metal rack, and suspended in a Napco E series Model 5831 vacuum oven at ambient temperature under a vacuum of 30 in. Hg for 24 h for further drying. The temperature in the oven was then increased and kept at 100 °C for 5–6 days. The resulting films were ~ 0.08 mm (3 mils) thick.

The glass transition temperature of the dried film was measured and compared with a sample of PS powder taken directly from the Pressure Chemical bottle. The glass transition temperature was determined by a Perkin-Elmer differential scanning calorimeter System-4 at a rate of 20 °C/min, in the temperature range 70–130 °C. If the glass transition temperature of the film was less than that of the original powder, the film was further heated in the oven until the two temperatures matched. This procedure was necessary to avoid plasticization of the film by residual solvent and hence ensure proper relaxation behavior.

Strips 0.75 in. long and 0.25 in. wide were cut from the film sample with a fresh razor. Strips of paper were subsequently wrapped around each end of the sample and bound by self-adhesive labels of the same size. This is done to ensure that the grips used to pull the sample would not slip over the surface during stretching. A line was drawn with a nonpermanent marking pen across part of the middle of each sample to check for uniformity in stretching after completion of the experiment.

Mechanical and Infrared Measurements. Simultaneous measurement of sample modulus and orientation requires the construction of an apparatus that is capable of measuring stress-strain-time data and that could be moved into the sample chamber of an IR apparatus where orientation relaxation could be monitored. Such an apparatus is shown schematically in Figure 3. Here, stress and strain are measured by a Sensotec

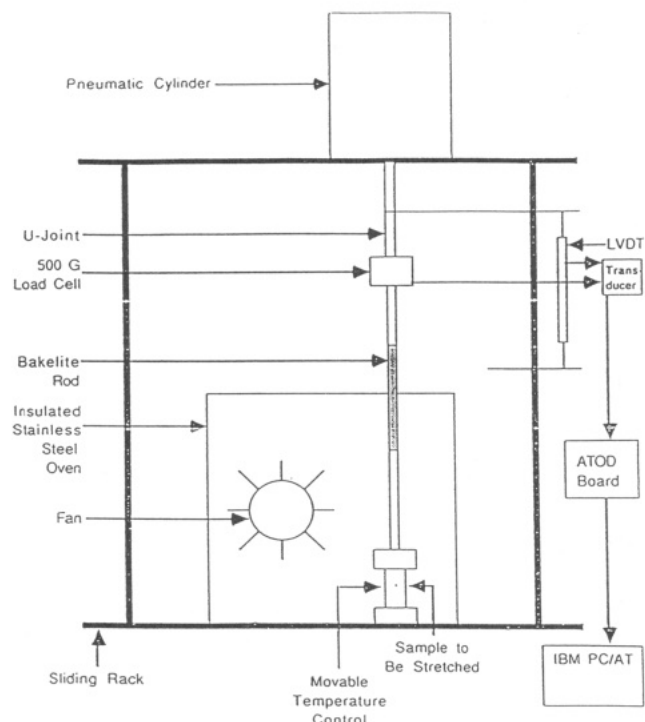


Figure 3. Schematic of the dynamic infrared apparatus.

Model BL431 500-g-load cell and a Transtek Model 246-000 linear velocity displacement transducer (LVDT), respectively. The analog signal from the load cell is transferred to a Sensotec Model GM signal conditioner and digital readout, while the LVDT analog signal is transferred to a Transtek Model 1002 transducer indicator with digital readout. Both indicators are equipped with adjustable zero and gain to assure proper measurement. Analog signals from these two components are then transferred to an IBM PC/AT via an IBM PC 12-bit 4-channel data acquisition and control adapter. They are then digitized by a data acquisition program.²²

Before data could be acquired, the program requires the determination of the top grip tension. The top grip is constructed of a 6.25-in. piece of hollowed aluminum, a 3-in. piece of Bakelite, and a 9-in. piece of hollowed aluminum that includes the top grip. Before the grip is placed in the oven, the chamber is equilibrated to 125 °C, via a Digi-Sense Model 2168-80 proportional temperature controller with a K-type thermocouple, which regulates the temperature in the sample vicinity. Temperature in the sample vicinity is likewise monitored by several J-type thermocouple probes surrounding the sample area. The oven is constructed of 316 stainless steel. This includes 0.5-in.-thick plates for the front, back, and top plates of the chamber, and 0.875-in.-thick side plates where the heater cartridges are located. The outside of the chamber is insulated with a 0.5-in.-thick sheet of asbestos.

After the top grip tension is measured, the chamber is opened and the sample is placed between the grips and tightened with a nut driver. The oven is then closed and the setup is carefully moved into the sample chamber of the Nicolet 7199 1180E FTIR apparatus via an overhead gantry system, until the infrared beam passes through the sample windows. The oven is equipped with 0.125-in. KBr windows on either side of the chamber to ensure transmittance of the infrared beam without absorption other than from the sample. Once the chamber reaches the set temperature, unpolarized and polarized spectra are taken of the sample to determine if any initial orientation exists. After the tension is again measured, the sample is ready to be stretched.

Rapid stretching to a constant strain is achieved by letting 1 psi air through the pneumatic cylinder on top of the setup, which lifts the top grip by a constant distance while the bottom grip in the oven remains stationary. Draw ratios of 2.2 are achieved in ~1 s. To simultaneously measure orientation and stress, the data acquisition program is started, the air pressure handle is lifted to stretch the film to a constant draw ratio of 2.2, and the

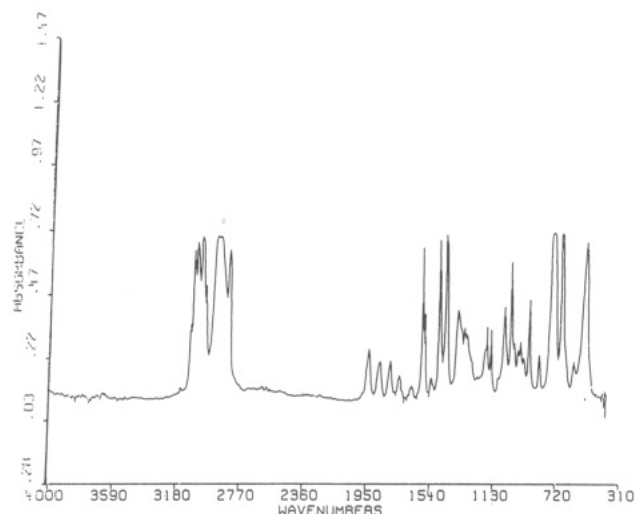


Figure 4. Infrared spectrum of fully hydrogenated polystyrene film.

IR scanning begins. Stress-strain-time data points are taken at a rate of 2 data points/s for the first 6 min of each run, after which they are taken at a rate of 1 data point/min until the completion of relaxation.

The infrared spectra for orientation analysis are collected with a Nicolet 7199 1180E spectrometer at 4-cm⁻¹ resolution (NDP = 4096 data points, NTP = 8192 transform points). The polarized spectra are obtained with a Spectra Tech ZnSe 25-mm-diameter polarizer. The measurement time for each spectral averaged polarized spectrum during relaxation is approximately 15 s (NSS = 16). Adequate interferogram signals require a gain of 16 for unpolarized spectra and 32 for polarized spectra.

At the completion of relaxation, the stretched sample is taken out of the oven and the oven is again equilibrated to 125 °C. The top grip weight is again measured to assure that no drift in tension occurred during the experiment. At this time, background spectra are also taken at 125 °C with the same gain and number of scans as the sample spectra for Fourier processing.

Experimental Data Analysis. The modulus data are reduced in the following manner. The modulus data generated by the data acquisition program are normalized with respect to the highest value. If drift occurs in the stress during the experiment (usually small, of the order of 1–2%), a linear drift in tension is assumed between the top grip tension measured at the beginning and end of the experimental run, and the appropriate values are subtracted from the tension measured during stretching before the modulus is calculated.

The infrared spectral analysis was done in the following manner. Three hydrogen stretching bands were chosen for analysis of the fully hydrogenated sample (HPS) with $M = 233\,000$, and six bands were chosen for analysis of the centrally deuterated polystyrene sample (HDH) with $M = 173\,700$. These include the 2850 cm⁻¹ (CH₂ symmetrical stretching vibration), 2925 cm⁻¹ (CH₂ asymmetrical stretching vibration), and the series of CH aromatic stretching bands around 3000 cm⁻¹ (3005, 3027, 3059, and 3085 cm⁻¹), as shown in Figure 4. For the triblock HDH polystyrene, the same protonated bands discussed above are analyzed in addition to their deuterated analogues at 2100 cm⁻¹ (CD₂ symmetrical stretching vibration), 2195 cm⁻¹ (CD₂ asymmetrical stretching), and the two aromatic CD stretching bands at 2273 and 2287 cm⁻¹ (Figure 5).

The spectra were generated by taking the ratio of the sample spectrum to the background single-beam spectrum after each interferogram was Fourier transformed. The absorbance was determined by integrating the areas under the bands. The integration program first finds the two minima in the band, a Lorentzian curve fitting routine interpolates between the digitized points offered by the Fourier analysis, a base-line correction is achieved by generating a straight line between the two minima and subtracting the values from the band, and the area integration proceeds by using Simpson's rule.

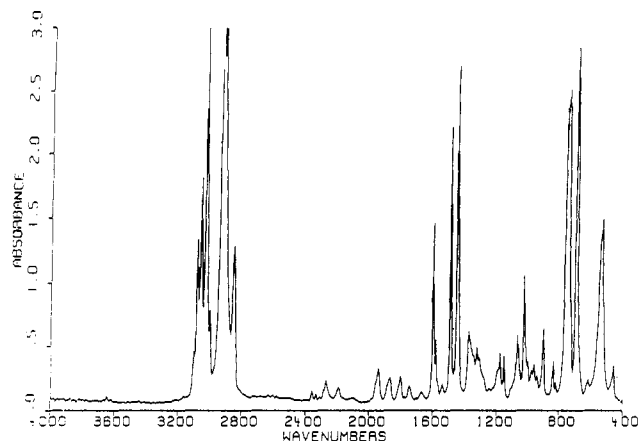


Figure 5. Infrared spectrum of centrally deuterated polystyrene triblock film.

Areas for each band are averaged over 10 spectra taken in time throughout the relaxation period. The Hermans orientation function is calculated as shown in the previous theory section, with one exception. The orientation function is normalized to the modulus value achieved at the time the first orientation point is calculated. A match between normalized orientation and modulus is thus forced at the beginning of the orientation data acquisition. This procedure was not found to create propagating errors in the analysis. A detailed error analysis is presented in ref 22.

Results

Film Thickness and Dynamic Range. The single polarization method chosen for analysis of the orientation data requires constant film thickness during stress relaxation at constant strain. At constant strain, constancy in film thickness is expected but minor changes in thickness could occur. The initial unstretched film thickness was ~ 0.08 mm (3 mils). Assuming constant volume during deformation, the thickness at a draw ratio of 2.2 is ~ 0.06 mm (2 mils). Constancy in film thickness and spectral data is checked by stretching films to a constant strain identical with those chosen for orientation modulus relaxation experiments and measuring the resulting unpolarized absorbance with time. A typical result for such an experiment is shown in Figure 6, where the hydrogenated polystyrene sample was stretched to a draw ratio of 2.2. As can be seen for the 3000-cm^{-1} band, the unpolarized absorbance fluctuates between values of 2.7 and 2.8. This is compared to a single perpendicular polarization experiment where absorbance values for the 3000-cm^{-1} band decrease from a value of 3.6 to 2.7. The relatively constant unpolarized absorbance with time after initial stretching implies a relatively constant film thickness, which is to be expected for a constant strain experiment. Figure 6 also provides a measure of the dynamic range of the polarized absorbance experiment and its sensitivity to measuring small changes in orientation.

HPS Orientation-Modulus Relaxation. The fully hydrogenated (HPS) monodisperse molecular weight polystyrene films ($M = 233\,000$) were stretched to a draw ratio of 2.2 at 125°C . This draw ratio was found to be appropriate in terms of providing a sufficiently strong polarization measurement while minimizing nonlinear effects, which occur at higher draw ratios. A maximum draw ratio of ~ 4 is required to strain harden the slack between entanglements in PS. The normalized orientation data for the 2925-cm^{-1} and 3000-cm^{-1} bands are compared to the normalized film bulk modulus in Figures 7 and 8, respectively. These data represent typical single-run

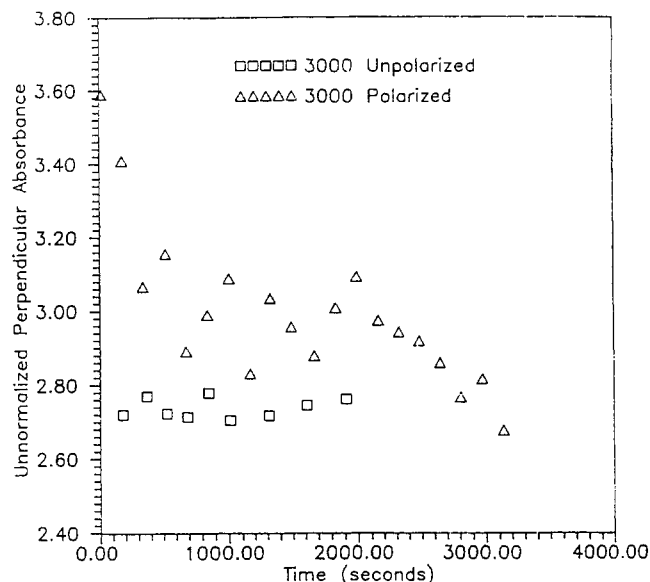


Figure 6. Comparison of the polarized and nonpolarized intensities of the 3000-cm^{-1} band in a polystyrene film subjected to a constant step draw ratio of 2.2 at 125°C .

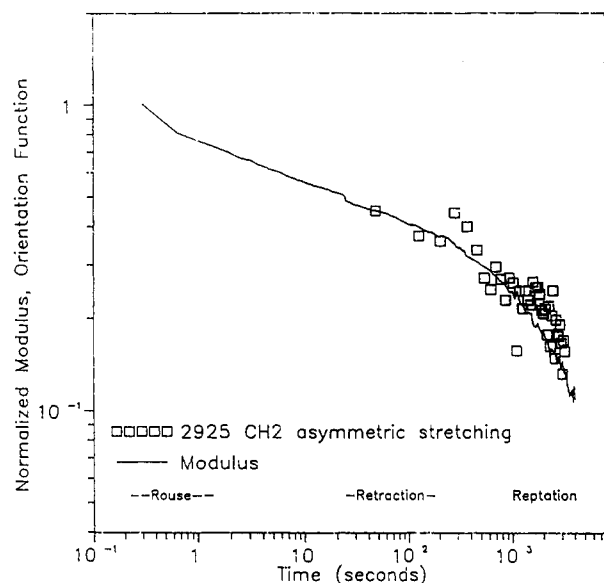


Figure 7. Relaxation of the modulus and orientation function of the 2925-cm^{-1} CH_2 stretching band in polystyrene HPS with $M = 233\,000$. The constant draw ratio of 2.2 was applied at 125°C .

experiments, which were repeated several times.

The time ranges for the Rouse entanglement relaxation τ_a , chain retraction (Rouse) τ_b , and reptation τ_c relaxation regions are indicated on the time axis. The reptation time was calculated from diffusion data of Kramer et al.^{23,24} and Whitlow and Wool²⁵ by using

$$\tau_c = \langle R^2 \rangle / 3\pi^2 D \quad (9)$$

where $\langle R^2 \rangle$ is the mean-square end-to-end vector and D is the self-diffusion coefficient. Equation 9 reduces to

$$\tau_c = 1.54 \times 10^{-18} M / D \text{ (s)} \quad (10)$$

where M is the molecular weight and the diffusion coefficient is expressed in units of cm^2/s . Whitlow and Wool, using SIMS, obtained $D = 5.6 \times 10^{-16} \text{ cm}^2/\text{s}$ for $M = 103\,000$ at 125°C , which gives $\tau_c = 283$ s. Correcting for molecular weight with $\tau_c \sim M^3$, the reptation time for $M = 233\,000$ is $\tau_c = 3280$ s. Green and Kramer, using FRES, obtained $D = 3.5 \times 10^{-16} \text{ cm}^2/\text{s}$ for $M = 110\,000$

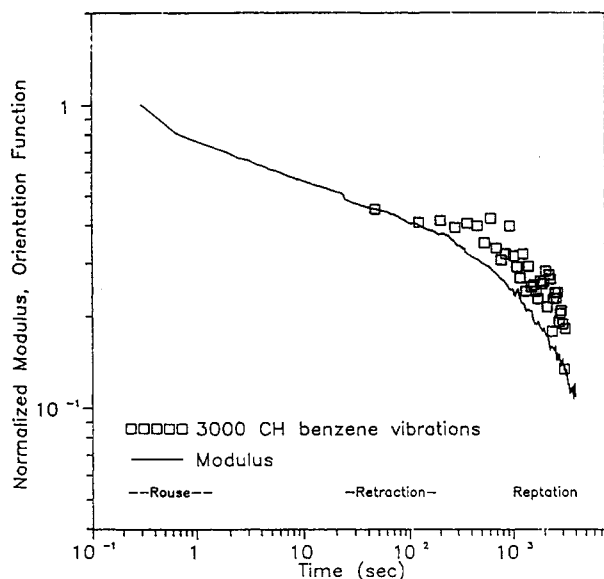


Figure 8. Relaxation of the modulus and orientation function of the 3000-cm⁻¹ aromatic CH stretching band in polystyrene HPS with $M = 233\,000$. The constant draw ratio of 2.2 was applied at 125 °C.

Table II
Polystyrene Relaxation Times at 125 °C

polymer	$M \times 10^{-3}$	τ_a , s	τ_b , s	τ_c , s	τ_d , s
HDH	75	0.5	9	109	9
HPS	103	0.5	17	283	42
HDH	173.7	0.5	47	1348	371
HPS	233	0.5	85	3280	1147
HPS	400	0.5	247	16461	7795

at 125 °C, which gives $\tau_c = 4600$ s for $M = 233\,000$. These values are in reasonable agreement.

The Rouse time τ_a is related to the retraction time τ_b and the reptation time τ_c via^{2,7}

$$\tau_c = 3N\tau_b = 3N^3\tau_a \quad (11)$$

where $N = M/M_e$ and M_e is the critical entanglement molecular weight. Letting $N = 233\,000/18\,000 = 13$, and using a reptation time of 3280 s, we obtain the retraction time $\tau_b = 85$ s and the entanglement relaxation time $\tau_a = 0.5$ s. These values are in close agreement with values obtained by both Boue et al.⁴ and Monnerie et al.³ The relaxation times for all samples are given in Table II.

The mechanical viscoelastic relaxation time, τ_d , is expected to be shorter than the reptation time obtained from diffusion data. By use of Doi's approximation for τ_d based on chain length fluctuation⁸

$$\tau_d = \tau_c \{1 - 1.47[M_e/M]^{1/2}\}^2 \quad (12)$$

with $M_e = 18\,000$, we obtain $\tau_d = 1147$ s when $\tau_c = 3280$ s. From Figures 7 and 8, the orientation function at τ_d is ~ 0.25 , which is close to $1/e$.

While the orientation data in Figures 7 and 8 were not measured in the initial Rouse entanglement relaxation region in the first 10 s, the data are adequate in the retraction and reptation regions to draw some conclusions. Nearly complete orientation loss as well as bulk modulus loss occurs in the reptation region. Since the orientation and bulk modulus loss occurs well within the region theoretically designated for pure reptation, mechanisms such as constraint release, chain length fluctuations, and tube relaxation, which quicken the onset of reptation, cannot be distinguished under these experimental conditions. Also, nearly complete relaxation of the mechan-

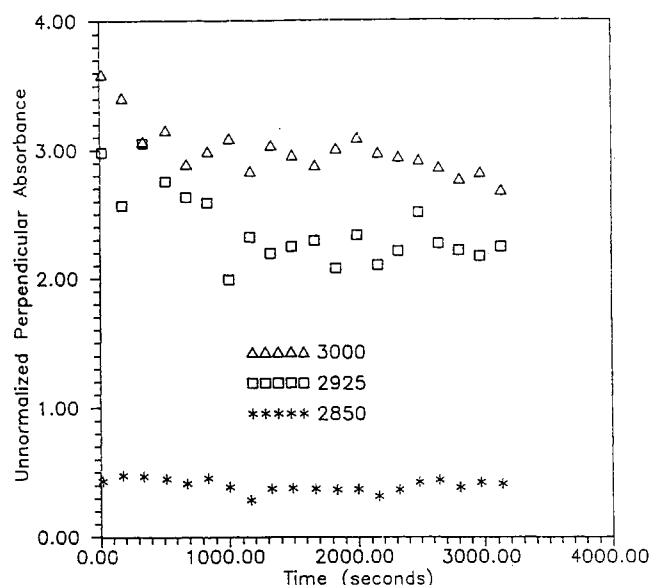


Figure 9. Comparison of the change in polarized absorbance intensity of the CH stretching bands in polystyrene at a draw ratio of 2.2. HPS with $M = 233\,000$.

ical and orientation function data occurs in the vicinity of the diffusion reptation time at 3280 s.

The orientation data for the 2925-cm⁻¹ band in Figure 7 seem to lie slightly above the modulus curve. This effect is more pronounced in Figure 8 for the 3000-cm⁻¹ band. Lack of complete coincidence of the optical and mechanical data in these figures suggests nonlinearity in the stress-optical rule. The measured nonlinearity occurs at stress levels under approximately 87 psi. This stress level is less than 145 psi, which is the stress predicted by Matsumoto and Bogue²⁶ as necessary for the onset of nonlinearity in constant shear rate experiments. Since stress levels of approximately 200 psi occur during initial stretching; however, residual orientation from the earlier strain hardening stress level may be "remembered" by the melt at later times. Positive deviations of the stress optical coefficient (SOC) in Figure 8 could be argued to favor nematic orientation effects such that released chain end segments (from the tube) "absorb" on the oriented surrounding matrix and contribute additional orientation but little stress. However, nematic ordering on its own would make the orientation relaxation time appear longer than the diffusion relaxation time, which is not seen in the data.

The 2850-cm⁻¹ band was not analyzed due to its relative insensitivity in measuring orientation in uniaxial stretching and subsequent relaxation. This can be seen in Figure 9, where representative data for the polarized absorbances (not normalized) are compared to each other for the respective bands. While the 2925- and 3000-cm⁻¹ bands show an appreciable fall in the polarized absorbance during relaxation, the 2850-cm⁻¹ band has little or no change in polarized absorbance, indicating its insensitivity and lack of dynamic range to measure the relaxation process. This band can be used to obtain useful orientation information at higher draw ratios and increased spectral averaging.^{17,18}

Centrally Deuterated Triblock HDH Relaxation. The centrally deuterated polystyrene HDH films ($M = 173\,700$) were stretched to a draw ratio of 2.2 at 125 °C. The normalized orientation data for the 2925- and 3000-cm⁻¹ bands (protonated chain ends) are compared to their deuterated analogues, 2195 and 2273 cm⁻¹ (chain center), as well as the normalized film bulk modulus in Figures 10 and 11, respectively. The Rouse, retraction, and reptation regions are again indicated on the time axis.

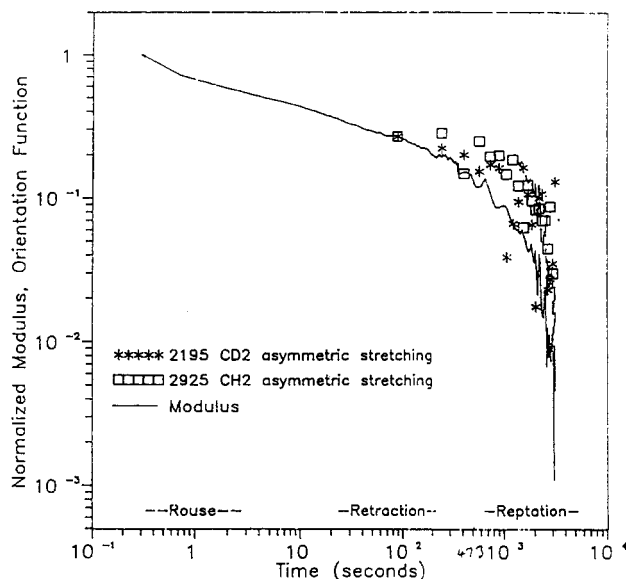


Figure 10. Relaxation of the modulus and orientation function of the 2195 (deuterated chain center) and 2925- cm^{-1} bands (protonated chain ends) in the HDH centrally deuterated triblock polystyrene sample, $M = 177\,000$. The constant draw ratio of 2.2 was applied at $125\,^{\circ}\text{C}$. The chain ends are seen to relax at about the same rate as the chain center.

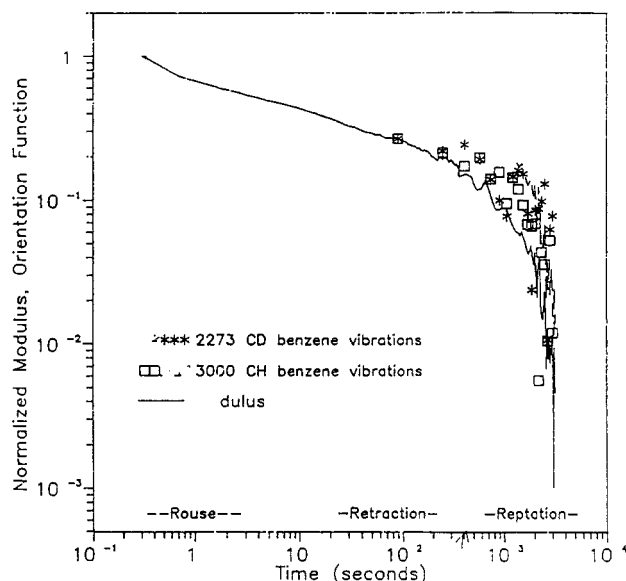


Figure 11. Relaxation of the modulus and orientation function of the 2273 (deuterated chain center) and 3000- cm^{-1} bands (protonated chain ends) in the HDH centrally deuterated triblock polystyrene sample, $M = 177\,000$. The constant draw ratio of 2.2 was applied at $125\,^{\circ}\text{C}$.

By use of diffusion data of Whitlow and Wool,²⁵ the relaxation times at $125\,^{\circ}\text{C}$ are obtained as follows: reptation time $\tau_c = 1360\text{ s}$, the retraction time $\tau_b = 47\text{ s}$, Rouse entanglement relaxation time $\tau_a = 0.5\text{ s}$, and mechanical relaxation time $\tau_d = 377\text{ s}$ (Table II).

The terminal relaxation region occurs in the vicinity of the theoretical reptation time. However, the orientation loss in the centrally deuterated portion of the polymer molecule is nearly equivalent to that of the protonated end portions in Figures 10 and 11. This result, which was reproduced many times, argues against a purely reptative mechanism dominating the relaxation process in the retraction/reptation region, where one expects the polymer chain ends to lose their orientation before the center of the chain.

The relaxation time for the chain ends in the symmetric triblock containing a chain end fraction $\phi_H = 0.64$ of protonated monomers and a center fraction $(1 - \phi_H)$ of deuterated monomers can be determined from the reptation model by the method of Kim and Wool²⁷ and Lee and Wool.¹⁷ The fraction of protonated chain ends, $F_H(t)$, remaining in the tube of the triblock HDH chain is given by

$$F_H(t) = 1 - 4/(\phi_H \pi^{3/2}) (t/\tau_c)^{1/2} \quad (\tau_b < t < \tau^*) \quad (13)$$

where τ^* is the time for the chain ends to relax to zero. At $F_H(t) = 0$, $\tau^* = 0.79 \tau_c$, such that for a reptation time of 1348 s , $\tau^* = 1070\text{ s}$. The relaxation time at $1/e$ for the chain ends occurs at $F_H(t) = 0.37$ such that $\tau(1/e) = 0.32 \tau_c = 427\text{ s}$. It can be seen from Figures 10 and 11 that the chain ends do not relax at $\tau = 1070\text{ s}$, but rather relax as the entire chain relaxes (as seen by the coincidence with the modulus and chain center data). The orientation function for all of the bands continues to remain slightly above the bulk modulus curve, as was seen in the completely hydrogenated case. This behavior indicates a similar deviation from the stress optical law response as noted for the fully hydrogenated PS in Figure 7 and 8.

The HDH experimental data differ with the results of Tassin et al.¹⁹ who deduced from their relaxation experiments on uniaxially deformed labeled polystyrenes HDH triblocks that the orientation relaxation of polymer chain segments depends on their location in the polymer chain. They investigated polystyrenes with $M_w = 188\,000$ and $502\,000$ with deuterated center and end segments with $M_w(D) = 30\,000$, approximately. The deuterated section represented $\sim 15\%$ of the chain with $M_w = 188\,000$ and $\sim 7\%$ for the higher molecular weight material. This compares with our HDH chains with 34% deuterated central section. Tassin et al. concluded that the chain end sections relaxed before the center section. Differences in experimental procedures and deuterated segment lengths may account for this discrepancy. The major experimental differences involve (a) use of a higher draw ratio, in the range 3–4, compared to our value of 2.2; (b) extraction of the modulus–orientation relaxation data by deconvolution of constant strain rate data compared to our direct relaxation data; (c) quench–start techniques compared to our in situ measurement of both stress and orientation; (d) WLF shifted piecewise data from experiments at several temperatures compared to our constant temperature data over the relaxation range; and (e) dual polarization versus single polarization in our experiments. As the labeled chain end length becomes shorter, the expectation is that the chain end sections should relax before the center. This is true for Rouse as well as reptation dynamics in diffusion processes. However, the mechanical relaxation process may permit other mechanisms to mask the dynamics associated with diffusion dynamics.

These HDH homopolymer results are in agreement in part with similar experiments by Koberstein et al.,²⁸ who examined HDH relaxation using modulated dynamic dichroism. The HDH results are also in agreement with flow birefringence studies of Osaki et al.³¹ They examined stress relaxation of a triblock copolymer made from PMMA–PS–PMMA (MSM), in 11% solution of polychlorinated biphenyl, subjected to a constant shear strain. The MSM triblock had a molecular weight of $1\,260\,000$ with a PS fraction of 0.4. Correcting M_e for concentration effects [$M_e(c) \approx 18000/0.11$], the entanglement density is such that $M/M_e(c) \approx 8$, which is roughly equivalent to the our HDH experiment with $M \approx 144\,000$. This method is analogous to the HDH system since the PS and PMMA

have different stress-optical coefficients. The anisotropic relaxation of this system should exhibit large and predictable deviations from the stress-optical law if reptation is the dominant mechanism of relaxation. Their results indicated that the change in birefringence with relaxation followed the stress-optic law, which was contrary to the predictions of both the Rouse and Tube models for this system. The constant stress-optical coefficient, which related the birefringence to the shear stress, was well approximated from the individual constants for PS and PMMA weighted to their mole fractions in the triblock. This further supports our finding that the HDH chains do not relax by a purely reptative process. Osaki et al. mentioned that their result was inconsistent with an earlier HDH dichroism relaxation study reported by Lee and Wool,⁷ who observed the HDH chain ends in a higher molecular weight matrix to relax before the center, as in pure reptation. In the next section, we show that this inconsistency is potentially explained in terms of matrix effects.

Matrix Effects on Triblock HDH Relaxation. Lee and Wool¹⁷ examined the relaxation of a centrally deuterated PS chain with $M = 75\,000$ in a high molecular weight matrix. They did not conduct the homopolymer HDH relaxation experiment because the low molecular weight material would not support the high draw ratios used to measure the orientation response. Instead, they diluted the low molecular weight HDH chains in a high molecular weight protonated matrix with $M = 233\,000$. They inferred that the protonated chain ends relaxed first before the deuterated chain center. They arrived at this conclusion by comparing the relaxation of the deuterated center of the triblock with the relaxation of an entirely deuterated chain of the same molecular weight as the triblock in the same $233\,000$ higher molecular weight matrix. Since the average relaxation of the entire deuterated chain in the matrix was faster than the deuterated center of the triblock, the ends of the triblock were considered to relax before the center.

We examined our HDH ($M = 173\,700$) triblock chains relaxing in a $400\,000$ fully protonated higher molecular weight matrix. The relaxation times of the HDH chain and the $400\,000$ chains were well separated by a factor of ~ 12 (Table II). Given that the HDH chain has a reptation relaxation time of 1348 s, the relaxation times for the matrix with $M = 400\,000$ are as follows; $\tau_c = 16\,461$ s, $\tau_b = 247$ s, $\tau_a = 0.5$ s, and $\tau_d = 7795$ s. The results shown in Figure 12 indicate that the centrally deuterated section of the chain relaxed more slowly in the matrix than in the homopolymer. Lee and Wool¹⁷ observed that the center of the HDH chain in the $233\,000$ matrix relaxed more slowly than the fully deuterated chain of comparable molecular weight in the same matrix. In both our experiment and the Lee and Wool experiments, the deuterated portion of the HDH triblock relaxes more slowly in a matrix of higher molecular weight, and in this sense, the experiments agree with each other.

Discussion

The reptation mechanism alone cannot explain the mechanical relaxation of the HDH homopolymer since the chain ends relax at the same rate as the chain center in the terminal relaxation region. The Doi-Edwards theory predicts a clear separation of chain end versus chain center relaxation. Similar relaxation rates could be consistent with constraint release processes where the topological constraints are relaxing at the same rate as the chain. Thus, in a higher molecular weight matrix, the constraints are relatively fixed for the HDH probe chain and the HDH

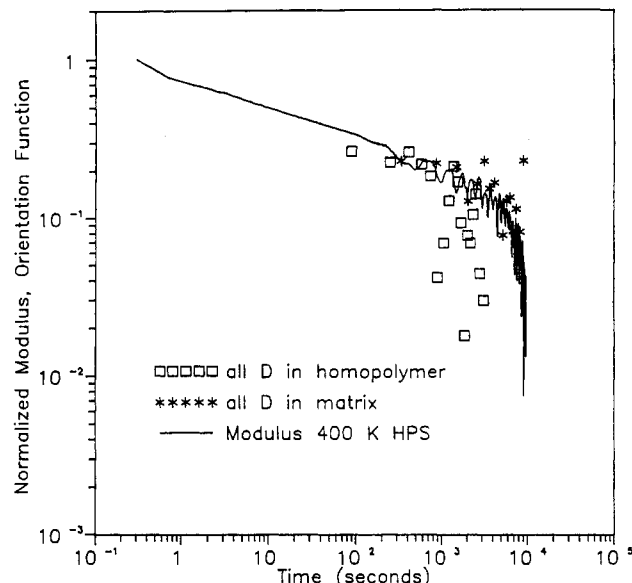


Figure 12. Comparison of the orientation relaxation of the centrally deuterated bands of the HDH triblock polystyrene chain in the homopolymer and in a matrix with $M = 400\,000$. The constant draw ratio of 2.2 was applied at 125°C . The chain center relaxes more slowly in the high molecular weight matrix.

center relaxes slower than the reptating chain ends compared to the homopolymer. Lee and Wool¹⁸ noted that the matrix molecular weight, P , had to exceed the deuterated probe chain molecular weight, M , before the relaxation rate of the probe chain became constant. Thus, the matrix P has a strong effect on the relaxation rate of probe chains for $M > P$ but little effect for $M < P$. If the matrix relaxes a chain by removing a topological constraint at random along the chain, then the probe chain has the ability to relax its orientation locally by an entanglement relaxation process. This would allow the probe chain to relax its center at the same rate as the ends. However, the details of constraint release processes and their effects on mechanical properties are unclear.

Des Cloizeaux's¹⁵ concept of double reptation could explain the HDH relaxation data. This approach allows for relaxation of two entanglements, one from each chain comprising the entanglement "couple", in the reptation disentanglement process. Thus, while a chain end disentangles from an entanglement at random position on the other chain, both sections relax their orientation. But since the other entanglement occurs at random along the chain, it could result in loss of orientation from both ends and center at similar rates.

Nematic orientation coupling could also be consistent with some of these data.²⁹⁻³¹ With the HDH homopolymer, it could be argued that the chain ends couple with the surrounding matrix and appear to have the same relaxation rate as the chain center. However, matrix relaxation experiments of Lee and Wool clearly show that the lower molecular weight probe chain does not have the same relaxation rate as the higher molecular weight matrix, although the rate is slowed compared to the homopolymer. Also, the nematic orientation process increases the relaxation time above the pure reptation process with zero coupling to the matrix. Polymer melt relaxation times are known to be shorter than the reptation times deduced from diffusion data. Nematic orientation alone would tend to increase rather than decrease the relaxation times.

The chain end fluctuation mechanism (CEF) contributes in the early region of the plateau, but should not effect the HDH results in the terminal region as depicted in Figures

10 and 11. By its nature it would tend to enhance the chain end relaxation above that of the chain center, which is not consistent with our data. It could be argued that the CEF mechanism is overshadowed by the constraint release mechanism in the HDH homopolymer experiments, even though it is independent of this mechanism.

The vector percolation network relaxation mechanism examined by Wool et al.¹⁴ in real networks could also explain the HDH and matrix relaxation data. Recent studies of the mechanical relaxation of two-dimensional nets with random bond removal indicated that the stress relaxation modulus G , as a function of the fraction of remaining bonds p , behaved as

$$G(p) = (p - p_c)^{\nu} \quad (14)$$

where p_c is the percolation threshold at which $G = 0$ and ν is the critical exponent. From stress relaxation experiments at constant strain on 20×20 cm networks containing ~ 2000 bonds, Wool et al. found that, with random bond removal, $p_c \approx 0.72$ and $\nu \approx 1.1$ – 1.5 . This means that only 28% of the bonds had to be removed before the stress at constant uniaxial strain relaxed to zero. The remaining 72% of the bonds relaxed in a cooperative process near p_c . This means that the majority of the bonds relaxed their elastic stress by a mechanism other than fracture. In three-dimensional networks, the vector percolation threshold is expected to be closer to 0.5, but the physics of the relaxation mechanism is essentially unchanged from the two-dimensional result. The higher p_c value observed for the network relaxation experiment is consistent with vector percolation but the low exponent ν is comparable with normal scalar percolation, as in conduction. The scalar percolation threshold was observed for fracture of the two-dimensional network; i.e., 50% of the bonds had to be randomly removed before the network could no longer sustain a constant load. The vector percolation threshold is higher than the scalar threshold because of the greater difficulty in propagating vectors through a partially connected lattice, compared with conduction where the electrons can easily follow a connected and tortuous random path near p_c .

For the HDH homopolymer experiment and polymer melts, the percolation relaxation analogy could apply as follows. In the terminal relaxation region, the chains form an entanglement network, which accounts for the plateau rubber elastic modulus, G_N^0 . As the chains reptate, entanglements are removed at random (ignoring local single-chain correlation) from the network. The elasticity of the network changes and entanglement segments at both the center and end segments of the chain that have not relaxed by reptation can relax in a cooperative manner. The cooperative relaxation process is complex and involves an interesting nonuniform stress distribution on the remaining entanglement bonds. Since the majority of the bonds relax by a mechanism that does not involve disentanglement, the chain centers could appear to have the same relaxation rate as the chain ends. Also, the relaxation time with percolation in the terminal region is shorter than the diffusion reptation time, τ_c . Related properties such as the zero shear viscosity, η , will be affected by the elastic percolation process. When the HDH chains are diluted in a higher molecular weight matrix, the percolation process is suppressed for the HDH chains by moving the elastic relaxation of the matrix to longer time scales. Since the high molecular weight entanglement matrix remains fixed on the time scale of the HDH relaxation, the dynamics of the single HDH chain should be observed. Thus, closer agreement with the reptation

predictions are observed in this case.

We have demonstrated elsewhere that the percolation mechanism is a valid method of describing elastic relaxation with random bond removal in real macroscopic networks. However, the relationship between such networks and relaxing entanglement networks formed from linear macromolecules needs to be further explored. If we admit the existence of entanglement networks with elastic properties in real polymer melts, then the physics of the percolation process should have application in describing their properties.

With regard to the experimental techniques, the following comments are offered. Although the single polarization dynamic infrared experiment is a viable one, several differential methods such as that described by Stein³² or Gotoh et al.³³ can be more accurate when low values of dichroism are encountered. Advances in liquid-crystal technology allow the continuous rotation of linearly polarized light from 0 to 90° and permit the easy measurement of difference spectra.³⁴ Modulated techniques, such as those developed by Noda et al.,³⁵ bring improvements in time resolution and sensitivity to those mentioned above.

Conclusions

Single polarization infrared spectroscopy has been used to investigate the orientation relaxation of step-strained polystyrene melts. The experimental apparatus was constructed in a manner to provide bulk film modulus and orientation relaxation measurements in situ.

Orientation-modulus relaxation was performed with two polystyrenes, HPS and HDH. When the relaxation of the monodisperse 233 000 molecular weight hydrogenated polystyrene (HPS) was investigated in its homopolymer melt, orientation relaxation occurred in the terminal relaxation region. However, the orientation function in some areas of the relaxation curve was slightly greater than the modulus in the retraction and reptation regions. This indicates nonlinearity in the stress-optical law at these strains.

When the same experiment was performed with a monodisperse centrally deuterated (HDH) 173 700 molecular weight polystyrene, the same orientation relaxation effects mentioned above were seen. In addition, the orientation function of the chain end sections (66% protonated) relaxed in the same manner as the chain center section (34% deuterated). This result appears to be contrary to the single-chain reptation prediction but is consistent with similar birefringence relaxation experiments on PS-PMMA-PS triblocks of Osaki et al. However, in a high molecular weight 400 000 matrix, the relaxation of the HDH chain center was much longer than in the homopolymer. This result was consistent with the reptation prediction, and further work needs to be done to separate dynamics from mechanical relaxation effects. Relaxation of entanglement networks by percolation was discussed as an additional mechanism to explain the data.

To further investigate the relaxation of chain segments in polymer melts, we are currently examining the interdiffusion behavior of HDH chains at HDH-HPS interfaces using neutron reflection.³⁶ The initial results indicate that the chain centers exhibit retarded diffusion compared to the entire chain at times up to $\sim 1/3$ of the relaxation time. These experiments will help to distinguish the role of the chain dynamics in melt diffusion and mechanical relaxation.

Acknowledgment. We are grateful to the National Science Foundation, Polymers Program, for financial

support of this work, under Grant DMR 86-11551. Support for the FTIR facility was provided by the Materials Research Laboratory, Center of Microanalysis of Materials, Department of Energy under Grant DE-AC 0276ER 01198.

References and Notes

- (1) Rouse, P. E. *J. Chem. Phys.* **1953**, *21*, 1272.
- (2) Doi, M.; Edwards, S. F. *J. Chem. Soc., Faraday Trans. 2* **1978**, *74*, 1789, 1802, 1818; **1979**, *75*, 38.
- (3) Merrill, W.; Tirrell, M.; Tassin, J.-F.; Monnerie, L. *Macromolecules* **1989**, *22*, 898.
- (4) Boue, F.; Nierlich, M.; Jannink, G.; Ball, R. C. *J. Phys. (Paris)* **1982**, *43*, 137.
- (5) Tassin, J.-F.; Monnerie, L. *Macromolecules* **1988**, *21*, 1846-1854.
- (6) Viovy, J. L. *J. Polym. Sci., Polym. Phys. Ed.* **1985**, *23*, 2423.
- (7) Viovy, J. L.; Monnerie, L.; Tassin, J. F. *J. Polym. Sci., Polym. Phys. Ed.* **1983**, *21*, 2427-2444.
- (8) Doi, M. *J. Polym. Sci., Polym. Phys. Ed.* **1980**, *18*, 1005, 1891, 2005.
- (9) De Gennes, P. G. *Chem. Phys.* **1971**, *5*, 55, 572.
- (10) Graessley, W. W. *Adv. Polym. Sci.* **1982**, *47*, 67.
- (11) Klein, J. *Macromolecules* **1978**, *11*, 853.
- (12) Klein, J. *Macromolecules* **1986**, *19*, 105.
- (13) Doi, M.; Pearson, D.; Kornfield, J.; Fuller, G. *Macromolecules* **1989**, *22*, 1488.
- (14) Wool, R. P. Presented at American Physical Society, March 1990. Wool, R. P.; Bernaert, Y.; Daley, M. A.; Agrawal, G. *Bull. Am. Phys. Soc.* **1991**, *36*, 792.
- (15) Des Cloizeaux, J. *Macromolecules* **1990**, *23*, 3992.
- (16) Lee, A.; Wool, R. P. *Macromolecules* **1986**, *19*, 1063.
- (17) Lee, A.; Wool, R. P. *Macromolecules* **1987**, *20*, 1924.
- (18) Lee, A.; Wool, R. P. *Polym. Prepr. (Am. Chem. Soc., Div. Polym. Chem.)* **1987**, *28* (1), 38; *Macromolecules*, submitted for publication.
- (19) Tassin, J. F.; Monnerie, L.; Fetters, L. J. *Macromolecules* **1988**, *21*, 2404.
- (20) Lefebvre, D.; Jasse, B.; Monnerie, L. *Polymer* **1983**, *24*, 1240.
- (21) Lantman, C. W.; Tassin, J. F.; Sergot, P.; Monnerie, L. *Macromolecules* **1989**, *22*, 483.
- (22) Walczak, W. J. M.S. Thesis, University of Illinois, Urbana IL, 1989.
- (23) Green, P. F.; Mills, P. J.; Palstrom, C. J.; Meyer, J. W.; Kramer, E. J. *Phys. Rev. Lett.* **1984**, *53*, 2145.
- (24) Green, P. F.; Kramer, E. J. *Macromolecules* **1986**, *19*, 1108.
- (25) Whitlow, S. J.; Wool, R. P. *Macromolecules* **1989**, *22*, 2648.
- (26) Matsumoto, T.; Bogue, D. C. *J. Polym. Sci., Phys. Ed.* **1977**, *15*, 1663.
- (27) Kim, Y.-H.; Wool, R. P. *Macromolecules* **1983**, *16*, 1115.
- (28) Koberstein, J., private communication of results obtained by B. D. Lawrey, Ph.D. Thesis, Princeton University, 1989.
- (29) Erman, B.; Jarry, J. P.; Monnerie, L., to be submitted for publication.
- (30) Kornfield, J.; Fuller, G.; Pearson, D. *Macromolecules* **1989**, *22*, 1334.
- (31) Osaki, K.; Takatori, E.; Ueda, M.; Kurata, M.; Kotaka, T.; Ohnuma, H. *Macromolecules* **1989**, *22*, 2457.
- (32) Stein, R. S. *J. Appl. Polym. Sci.* **1961**, *5*, 96.
- (33) Gotoh, R.; Takenakda, T.; Hayashi, S. *Kolloid Z.* **1965**, *205*, 18.
- (34) Schadt, M.; Helfrich, W. *Appl. Phys. Lett.* **1971**, *18*, 127.
- (35) Noda, I.; Dowrey, A. E.; Marcott, C. J. *J. Polym. Sci., Polym. Lett. Ed.* **1983**, *21*, 99.
- (36) Zhang, H.; Agrawal, G.; Wool, R. P.; Dozier, W. B.; Felcher, G.; Russell, T. P. *Macromolecules*, in press.